ISSN 1027-5495. Functional Materials, 29, No.1 (2022), p. 135-143.
doi:https://doi.org/10.15407/fm29.01.135

Effects of graphene oxide on durability of ultra high performance concrete

Luo Yeke[1], *YU Zhouping*[2]

[1]Zhejiang Industry Polytechnic College, 312000 Shaoxing, China
[2]Shaoxing University Yuanpei College, 312000 Shaoxing, China
[3]College of Civil Engineering, Changsha University of Science and Technology, 410076 Changsha, China

Received February 2, 2022

In this study, the effects of graphene oxide (GO) content on the mechanical property, durability, and drying shrinkage of Ultra-high performance concrete (UHPC) for Bridge were investigated, and corresponding microstructure evolution was also analyzed. The results showed that the flexural strength and compressive strength of UHPC with addition of GO were increased by 10.6 % ~ 25.7 % and 6.3 % ~ 15.8 % on day 28, respectively, and the optimum content of GO was 0.04 %. The chloride ion permeability and freeze-thaw resistance of UHPC increased with GO addition. The drying shrinkage of UHPC sample containing GO after 91 days increased by 1.4 % ~ 8.1 %. Microstructure analysis confirmed that the incorporation of GO into UHPC could improve its microstructure and pore distribution, in which the total porosity decreased by 16.6 % ~ 33.8 %, and the porosity (at the pore size of 0 ~ 20 nm) increased by 1.8 % ~ 8.6 %, respectively. This might be related to the nucleation effect of GO, the formation of dense gel structure between microcracks and GO, and the formation of hydrogen bonds between GO functional groups and C–S–H gels.

Keywords: ultra high performance concrete, graphene oxide, durability, microstructure.

Вплив оксиду графену на довговічність бетону з надвисокими характеристиками. *Luo Yeke, YU Zhouping*

Досліджено вплив вмісту оксиду графену (GO) на механічні властивості, довговічність та усадку при висиханні надвисокоякісного бетону (UHPC) для мостів. Проаналізовано відповідну еволюцію мікроструктури. Результати показали, що міцність на вигин та міцність на стиснення UHPC з додаванням GO збільшилися на 10,6–25,7 % та 6,3–15,8 % за 28 днів відповідно, а оптимальний вміст GO становив 0,04 %. Проникність іонів хлору та стійкість до заморожування та відтавання UHPC збільшувалися при додаванні GO. Усадка при висиханні зразка UHPC, що містить GO, через 91 день збільшилася на 1,4–8,1 %. Аналіз мікроструктури підтвердив, що включення GO в UHPC може поліпшити його мікроструктуру та розподіл пір, у яких загальна пористість зменшилася на 16,6 % ~ 33,8 %, а пористість (при розмірі пір 0 ~ 20 нм) збільшилася на 1,8 % ~ 8,6 % відповідно. Це може бути пов'язано з ефектом зародка утворення GO, утворенням щільної гелевої структури між мікротріщинами та ОГ, а також утворенням водневих зв'язків між функціональними групами GO та гелями C–S–H.

1. Introduction

By 1994, Larrard [1] first introduced the concept of ultra-high performance concrete (UHPC), which was favored due to its ultra-high strength, excellent toughness, and very low porosity and low permeability [2, 3]. In building structures, bridges, and roads, the use of UHPC as a protective layer for bridge concrete can reduce erosive damage from external corrosive ions through surface hardening technology. In contrast, the

use of UHPC for structural members of bridges can reduce the self-weight of the structure and improve the durability and service life of the structure. Although UHPC has many outstanding properties, it also has certain defects, such as the cementitious material content being about 800–1000 kg/m^3, high heat of hydration, poor fluidity, and easy shrinkage and cracking. Therefore, improving the workability and reducing the cracking of UHPC for bridges while ensuring its mechanical properties and durability has become a hot topic of interest for scholars.

Nanomaterials are recognized for their application in cementitious composites to improve the toughness, flexure, tensile, and durability of UHPC at the nanoscale. Among all the nanomaterials, carbon nanotubes, graphene-derived materials, carbon nanofibers, and nanosilica are well studied, while graphene oxide (GO) is considered one of the most promising nanomaterials for improving the mechanical properties and durability of UHPC. This is due to the hydrophilic nature of GO, which is easily dispersed in water and can cost-effectively improve the performance of UHPC. In [5] it is reported that the addition of 0.05 % GO increased the compressive strength and flexural strength of cement mortar by 15–33 % and 41–58 %, respectively, which may be due to the interlocking and interactive inhibition of crack development between microcracks and GO, as well as the contribution of GO to facilitation of the hydration process by the formation of strong interfacial forces between the carboxyl groups on its surface and the hydration products. In [6] it was observed that the compressive strength, flexural strength, and tensile strength of cement mortar increased by 38.9 %, 60.7 %, and 78.6 %, respectively, when the dose of GO was 0.05 %, indicating the key role of GO in improving the strength of mortar. Authors of [7, 8] reported that the addition of GO enhanced the resistance of mortar to chloride ion penetration, carbonation, and freeze-thaw cycles, which was mainly attributed to the micro aggregate filling effect of GO and provided additional nucleation sites for cement hydration and regulated the crystal morphology of hydration products [9–11]. However, in [12] it was found that when the amount of GO exceeds the optimum amount, the mechanical properties of the cementitious material decrease due to agglomeration phenomena.

With the development of nanotechnology, GO can be prepared industrially, reducing the cost of the GO use. In addition, the incorporation amount of GO in cement-based materials is also very low. Therefore, the application of GO in cementitious materials has good economic performance. However, previous studies have mainly focused on the effects of GO on the properties of cement mortar and ordinary concrete, while relatively little research has been done on the effects of GO on the properties of UHPC. Thus, in this article, the effects of different doses of GO on the flexural strength, compressive strength, chloride ion penetration resistance, freeze-thaw resistance, and drying shrinkage of UHPC are investigated. Since UHPC is used in bridge engineering to make the bridge structure tend to be lighter and thinner, solving the problems of high self-weight, poor durability and easy cracking of traditional concrete bridge structures is urgent. In addition, the evolution of the porous structure of the HCFC with GO was studied by scanning electron microscopy (SEM) and the mercury pressure method (MIP).

2 Experimental

2.1 Raw materials

The cementing materials under study mainly include cement, silica fume and fly ash. The cement is P.O 52.5 ordinary Portland cement of Yangchun Cement Co., LTD., the silica fume is microsilica powder of Hengno Filter Material Co., LTD., and the fly ash is the first grade fly ash of HSBC new material. Fig. 1 shows the microstructure of cement, SF and FA; their chemical composition is shown in Table 1. The fine aggregate is the standard sand of Kezheng Instrument Co., LTD. The length and diameter of the steel fiber are 12 mm and 0.18–0.23 mm respectively. A water reducing agent is polycarboxylate superplasticizer (PS) made by Jiangsu Subert New Material Co., LTD. The solid content and the water reducing rate are 40 % and 25 % respectively.

GO was synthesized by the modified Hummers method [13]. The main parameters of GO are shown in Table 2. Fig. 2 shows the SEM image, the transmission electron microscope (TEM) image and the particle size distribution of GO. It can be seen from the figure that GO has a folded morphology, and its particle size is nanometer.

Table 1. The chemical compositions of cement, SF and FA (wt.%)

Chemical compositions	Al_2O_3	SiO_2	CaO	Fe_2O_3	MgO	SO_3	K_2O	Na_2O	L.O.I
Cement	5.98	20.56	64.72	3.08	1.39	3.01	0.72	0.16	1.23
SF	1.0	96.23	0.31	0.92	0.61	/	/	1.12	2.15
FA	7.24	73.02	18.76	0.05	0.15	/	0.04	0.21	

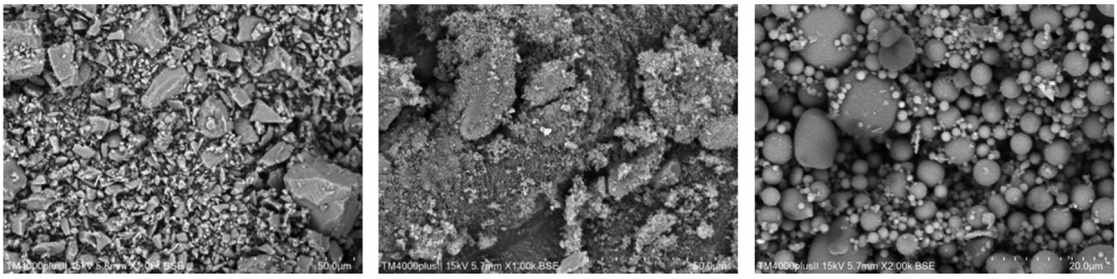

(a)Cement (b)SF (c)FA

Fig. 1. SEM of cement, SF and FA.

2.2 Design and preparation of the mixture

Four kinds of UHPC mixtures U-0, U-0.02 %, U-0.04 % and U-0.06 % were designed, which contained 0 %, 0.02 %, 0.04 % and 0.06 % GO in the cement mass respectively. The water-binder ratio of UHPC was 0.2, and the steel fiber content was 2 vol% in the sample. The fluidity of UHPC is kept in the range of 240–260 mm by adjusting the content of PS. The UHPC mixture ratios are shown in Table 3.

The preparation process of UHPC is shown in Fig. 3. First, cement, SF and FA were mixed and stirred for 1 min, the standard sand was added and stirred for 2 min, the the GO/PS solution prepared in advance was added (GO and PS were dissolved in water and sonicated for 30 min), and then the mixture was stirred for 2 min. Steel fiber was added and the mixture was stirred for another 3 min during this process. After the mixture was ready, it was poured into a mold, vibrated and finally molded. After the sample was molded, the mold was wrapped with plastic film, and the mold was removed after 24 h of indoor curing. The mold was placed in the standard curing room (temperature $T = 20\pm1°$, relative humidity > 95 %) for 28 days and 91 days.

2.3 Test method

According to the Test Method Standard for Fiber Reinforced Concrete (CECS 13:2009), the mechanical properties of UHPC should be tested according to the test requirements of Reactive powder Concrete (GB T 31387-2015). The sample size was 40×40×160 mm, and the loading rates of flexural strength and compressive strength were 50 N/s and 2.4 kN/s, respectively. The chloride ion permeability and freeze-thaw resistance of the samples were tested after curing for 28 days. The chloride ion migration coefficient of UHPC was measured according to the national standard GB/T 50082-2009. The sample had a cylindrical shape with a diameter of 100 mm and a thickness of 50 mm. The freeze-thaw resistance of 100×100×100 mm samples was tested, and the mass loss rate and dynamic modulus of UHPC samples were tested after 50 to 300 cycles. The drying shrinkage sample size of UHPC was 100×100×51.5 mm. After curing for 3 days under standard curing conditions, the specimen was placed in a curing room with a temperature of 22±1°C and relative humidity of 60±5 %. Then, the initial length of each sample was determined and the drying shrinkage of UHPC

Table 2. The physical and chemical properties of GO

Item	Mean diameter	Median diameter	Thickness	Carbon content	Oxygen content
GO	66.75 nm	62.25 nm	1–2 nm	47–60 %	50–55 %

Table 3. The mixture proportions of UHPC (kg/m^3)

Sample	Cement	SF	FA	Sand	Water	GO	PS
U-0	720	120	360	1320	240	0	36
U-0.02 %	720	120	360	1320	240	0.24	36
U-0.04 %	720	120	360	1320	240	0.48	36
U-0.06 %	720	120	360	1320	240	0.72	36

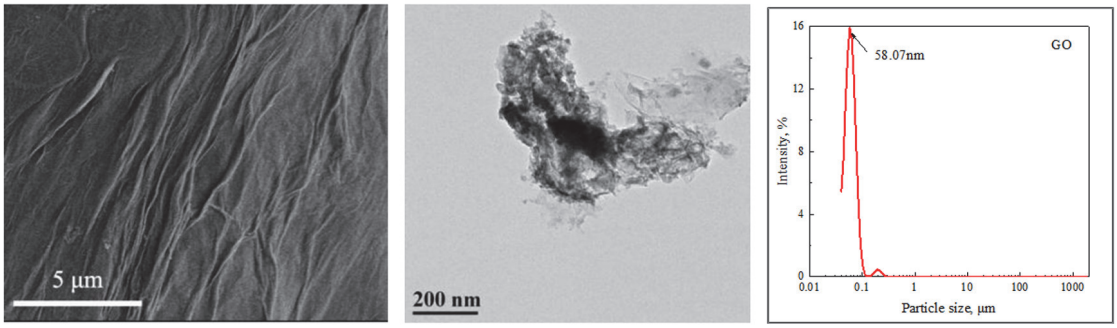

Fig. 2. The morphology of GO.

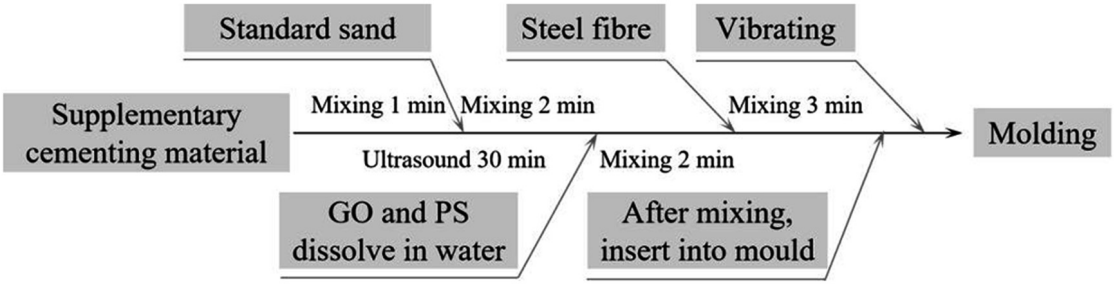

Fig. 3. Preparation process of UHPC.

was measured after 1, 3, 7, 14, 28, 56, and 91 days. The drying shrinkage test of the UHPC was repeated at least three times to ensure its accuracy.

The porosity and pore size distribution of UHPC were characterized by the mercury injection method (MIP). The size of the sample used for MIP testing was about 5 mm. Samples were selected from the UHPC sample as fragments with a size of about 10×10 mm with a flat surface. After spraying gold, the fragments were observed under scanning electron microscope.

3. Results and discussion

3.1 Workability

It can be seen from Fig. 4 that the swelling rate of UHPC tends to decrease with an increase in the GO doping. This is because the GO doping makes the water molecules adsorbed on the surface of GO particles and reduces the free water content, which leads to a serious decrease in the mobility of UHPC. When the degree of doping reaches 0.04 %, the change in swelling with an increase in GO doping is insignificant and amounts to approximately 1.5–4.5 %; when the degree of doping exceeds 0.04 %, the change in swelling of UHPC increases significantly, and the loss exceeds 10 %.

3.2 Mechanical properties

Fig. 5 shows the effect of GO incorporation on the flexural and compressive strengths of UHPC. The results show that the addition of GO improved the mechanical properties of UHPC. As shown in Fig. 5(a), the flexural strengths of the U-0.02 %, U-0.04 % and U-0.06 % specimens increased by 10.6 %, 25.7 % and 22.4 % after 28 days; 10.2 %, 24.1 % and 17.4 % after 91 days, respectively, compared with the baseline group. The compressive strength

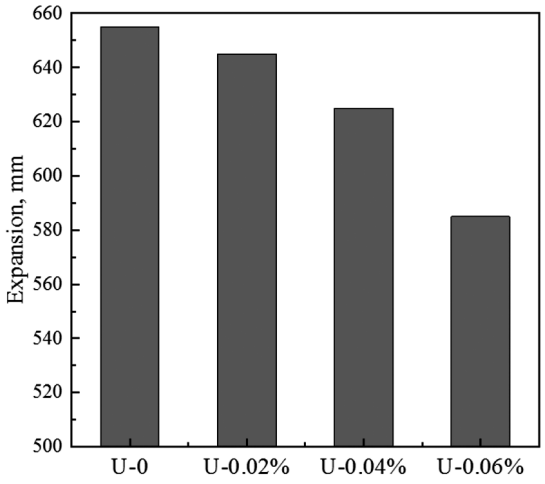

Fig. 4. Expansion test results.

after 28d and 91d increased by 6.3 %, 15.8 %, 11.3 % and 7.4 %, 16.7 %, 10.9 % for the specimens compared with the reference group. From the above, it can be seen that the mechanical properties of UHPC showed a trend of first increasing and then decreasing with an increase in the GO doping; and the optimum doping of GO in UHPC was 0.04 %, which was similar to the previous results. The enhancement of GO is mainly due to (1) the nucleation of GO, which can provide additional nucleation sites during the hydration of cement, thus improving the hydration of cement and the microstructure of UHPC [14, 15]; (2) the functional groups of GO improve the morphology of hydration products: GO can reduce the porosity of the crack budding stage, and the interaction between microcracks and GO can easily form a dense gel structure and inhibit the extension of cracks [16]; (3) the C–S–H gel layer of UHPC contains more calcium ions and hydroxides. Calcium ions bind to the oxygen-containing functional groups of GO, and water molecules form hydrogen bonds between GO functional groups and C–S–H gels [17].

3.3 Chloride ion infiltration

Fig. 6 shows the effect of GO doping on the chloride ion permeability of UHPC. It can be seen that the chloride mobility coefficients of the UHPC specimens containing GO after 28 d are lower than those of the reference group, which indicates that GO doping can reduce the chloride mobility coefficients of UHPC. The chloride mobility coefficients of the U-0, U-0.02 %, U-0.04 % and U-0.06 % specimens are $1.201 \cdot 10^{-12}$ m^2/s, $1.112 \cdot 10^{-12}$ m^2/s, $1.055 \cdot 10^{-12}$ m^2/s and $1.086 \cdot 10^{-12}$ m^2/s. The values $1.055 \cdot 10^{-12}$ m^2/s and $1.086 \cdot 10^{-12}$ m^2/s indicate that the chloride migration coefficient of UHPC does not decrease linearly with increasing GO doping, and similar results were obtained by Guo et al. [18]. When the GO doping degree was 0.04 %, UHPC exhibited the best resistance to chloride ion permeation with a 12.2 % reduction compared to the baseline group. This may be due to the fact that GO doping improved the microstructure of UHPC, reducing the number of macropores in the matrix and hindering the chloride ion transport in the pore channels.

3.4 Freeze-thaw resistance

Fig. 7 shows the effect of GO incorporation on the freeze-thaw resistance of UHPC. From the figure, it can be found that the

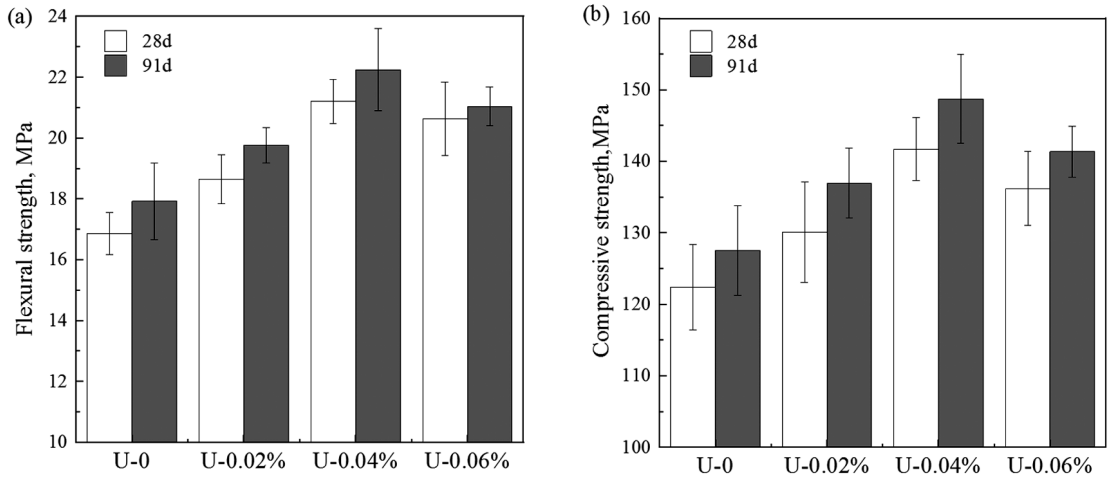

Fig. 5. The flexural strength and compressive strength of UHPC with different contents of GO.

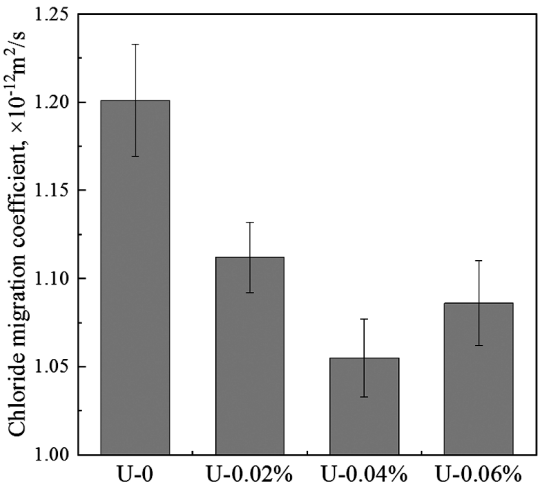

Fig. 6. Chloride migration coefficient of UHPC with various contents of GO.

mass loss rate of UHPC keeps increasing with an increase in the number of freeze-thaw cycles, but the relative dynamic modulus of elasticity shows a decreasing trend. As shown in Fig. 7(a), the mass loss of U-0.02 %, U-0.04 %, and U-0.06 % specimens was lower than that of the reference group, where the mass loss rate decreased by 15 %, 44 %, and 30.6 % after 300 freeze-thaw cycles, respectively, which indicated that the incorporation of GO improved the freeze-thaw resistance of UHPC. The mass-loss rate of UHPC was minimized when the GO incorporation amount was 0.04 %. As for the relative dynamic modulus of elasticity of UHPC, the relative dynamic modulus of elasticity of the specimens containing GO was higher than that of the reference group, which was U-0.04 % > U-0.06 % > U-0.02 % > U-0. In comparison to the reference group, the relative dynamic modulus of elasticity for the specimens U-0.02 %, U-0.04 %, and U-0.06 % increased by 5 %, 16 %, and 7.4 %, respectively, after 300 freeze-thaw cycles. This indicates that the relative dynamic modulus of elasticity of UHPC increases due to GO incorporation; the optimum amount of GO incorporation is 0.04 %, which is consistent with the results of Karim et al. [15].

3.5 Drying shrinkage

Fig. 8 shows the effect of GO incorporation on the drying shrinkage of UHPC. It is seen that the drying shrinkage of UHPC increased linearly in the early stage, and the growth rate decreased significantly after 28 d, while it stabilized in the later stage. The drying shrinkage rate of UHPC in the early stage is very close to that of the reference group, but with an increase in aging, the drying shrinkage rate of specimens containing GO is slightly higher than that of the reference group and basically follows U-0 > U-0.02 % > U-0.06 % > U-0.04 %. In comparison to the reference group, the drying shrinkage of the U-0.02 %, U-0.04 % and U-0.06 % samples decreased by 7.3 %, 17 % and 11.8 %, respectively, after 91 days. This indicates that the addition of GO reduced the drying shrinkage of UHPC, which is similar to previous results in the literature [19]. The effect of GO on the drying shrinkage of UHPC is explained by the mutual competition of two effects: the crystalline nucleation of GO promotes the hydration of the cement, forming more C–S–H gels to fill the

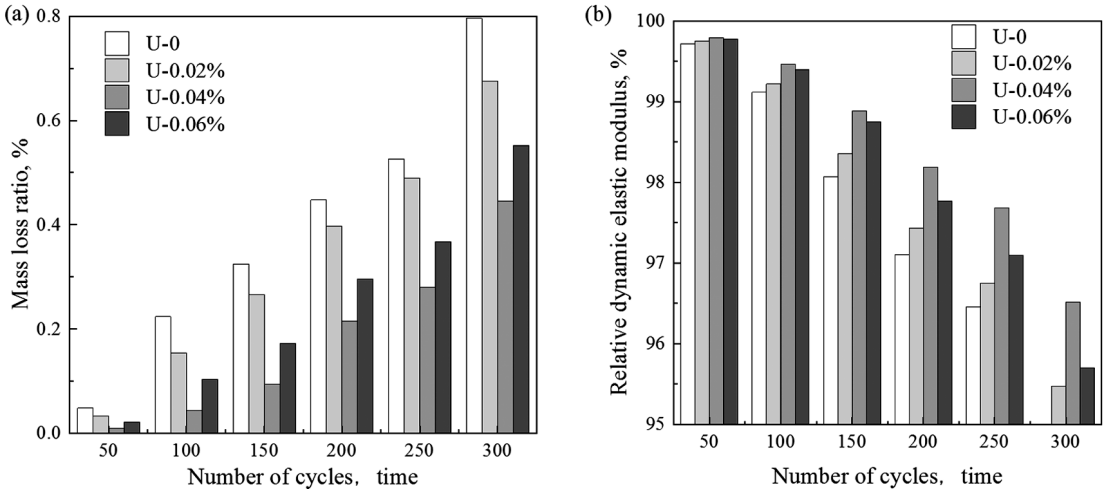

Fig.7. The mass loss ratio and relatif UHPC with different contents of GO.

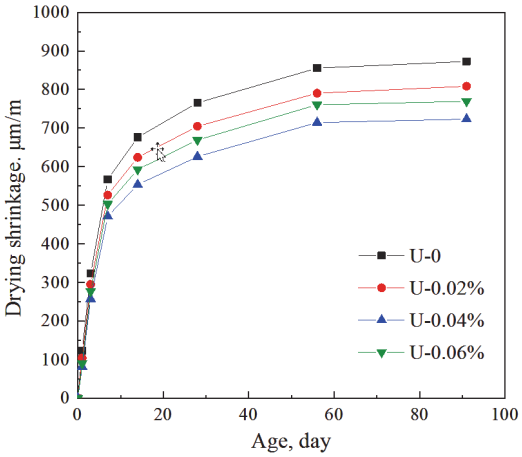

Fig. 8. Drying shrinkage of UHPC with different contents of GO.

macropores in the matrix and increasing the number of micropores [20], thus promoting the drying of UHPC shrinkage development. At the same time, the addition of GO changed the morphology of the hydration products, increased the density, reduced the evaporation of water inside the material, and hindered the expansion of microcracks in the matrix, thus reducing the shrinkage rate. The above results show that the shrinkage reducing effect of GO on UHPC is greater than the shrinkage increasing effect.

3.6 Mechanistic analysis

SEM analysis

Fig. 9 shows the SEM images of the UHPC specimens after 28 days. The figure shows that the main products of cement hydration mainly include C–S–H gel, CH crystals, and calcite. Low-density C–S–H gels and CH crystals are observed in Fig. 9(a), while microcracks may be related to the drying shrinkage of the matrix, which can negatively affect the mechanical properties and durability of UHPC. Uniformly distributed C–S–H gels and small amounts of CH crystals could be observed in the U-0.02 % and U-0.04 % specimens, and the gels were present as continuous composite layers in large amounts (Fig. 9b and c), which implies that the GO included in UHPC is a feasible reinforcing agent. However, when the GO doping was increased to 0.06 %, the number of pores in the specimens increased, and the density of the microstructure decreased (Fig. 9d).

MIP Analysis

The pore structure, especially the total porosity and pore size distribution, plays a crucial role in the performance of concrete. Currently, the mercury pressure technique is a widely used and effective method for evaluating cementitious materials [21]. According to Zhang [22], pores can be classified as harmless pores (0–20 nm), less harmful pores (20–50 nm), harmful pores (50–200 nm), and multi-harmful pores (>200 nm).

Fig. 10 shows the pore size distribution and cumulative porosity distribution in the UHPC specimens. It can be seen from the figure that the pore size distribution of UHPC specimens is mainly concentrated below 100 nm, which is related to its own compactness. The total porosity of UHPC specimens ranges from 0.0689 to 0.104 ml/g. Compared with the reference group, the total porosity of U-0.02 %, U-0.04 %, and U-0.06 % specimens decreased by 16.6 %, 33.8 %, and 25.9 %, respectively, indicating that the addition of GO reduced the porosity of UHPC. In general, pores larger than 200 nm in diameter have a very harmful effect on the strength of concrete, while pores smaller than 20 nm in diameter have a better effect on the shrinkage of concrete [23]. The content of pores (> 200 nm) in the U-0.02 %, U-0.04 %, and U-0.06 % specimens was reduced by 74 %, 70 %, and 82 %, respectively, compared to the reference group. The mechanism of the addition of GO promotes the hydration of the cement, increasing the content of C–S–H gel in the matrix to fill the large pores in the matrix. This explains why the addition of GO significantly improves the mechanical properties and durability of UHPC. In addition, the pore structure of UHPC specimens was refined with the addition of GO, and the porosity of 0–20 nm pore size increased with the addition of GO. Compared with the baseline group, the porosity of 0–50 nm pore size in the U-0.02 %, U-0.04 %, and U-0.06 % specimens decreased by 3.2 %, 19.1 %, and 10.4 %, respectively, while the reduction in the number of gel pores further confirmed that GO was beneficial to hinder the development of drying shrinkage of UHPC.

4. Conclusion

In this article, the effects of GO doping on the mechanical properties, chloride ion permeability, freeze-thaw resistance, and drying shrinkage of UHPC used for bridges were systematically analyzed, and the microstructure evolution of UHPC with different GO doping was also analyzed. Based on the results of the study, the following main conclusions were drawn:

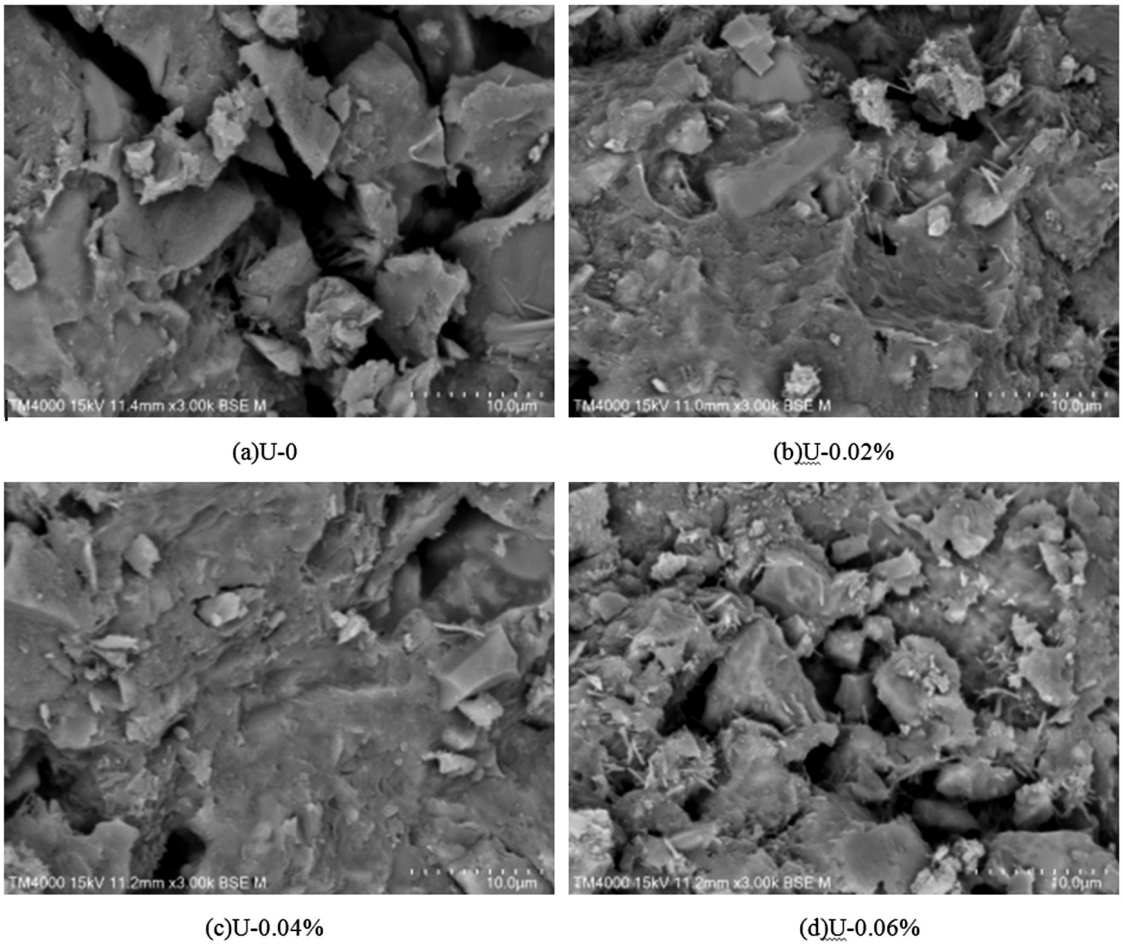

Fig. 9. SEM image of UHPC.

With an increase in the degree of GO doping, the rate of swelling of UHPC gradually decreases, and when the degree of doping reaches 0.04 %, the swelling rate changes less with an increase in the degree of GO doping and is approximately 1.5–4.5 %. Both the flexural and compressive strengths of UHPC showed a trend to increase and then decrease with increasing GO doping. Compared with the reference group, the flexural strength of UHPC specimens containing GO increased by 10.6 % ~ 25.7 % after 28 d, while the compressive strength increased by 6.3 % ~ 15.8 %. This indicates that the addition of GO can improve the mechanical properties of UHPC at the optimal dosage of 0.04 %.

The chloride ion mobility coefficients of U-0, U-0.02 %, U-0.04 %, and U-0.06 % specimens were $1.201 \cdot 10^{-12}$ m^2/s, $1.112 \cdot 10^{-12}$ m^2/s, $1.055 \cdot 10^{-12}$ m^2/s, and $1.086 \cdot 10^{-12}$ m^2/s, respectively, indicating that the addition of GO to UHPC can improve its resistance to chloride ion permeability.

After adding GO, the mass loss rate of UHPC specimens decreased by 15 % ~ 30.6 % after 300 freeze-thaw cycles, while the relative dynamic modulus of elasticity increased by 5 % ~ 16 %, indicating that the addition of GO significantly improved the freeze-thaw resistance of UHPC.

The drying shrinkage of UHPC basically followed the order of U-0 > U-0.02 % > U-0.06 % > U-0.04 %. The drying shrinkage of UHPC specimens containing GO after 91 days was reduced by 7.3 % ~ 17 %. This indicates that the addition of GO reduced the drying shrinkage of UHPC.

The total porosity of UHPC specimens ranged from 0.0689 to 0.104 ml/g. With the addition of GO, the total porosity of UHPC was reduced by 16.6 % to 33.8 %. More notably, GO refined the pores in UHPC, and the porosity of 0–50 nm pore size was reduced by 3.2 % ~ 19.1 %, respectively. This is consistent with the SEM images; thus, the doping of GO in UHPC can improve its microstructure and pore distribution.

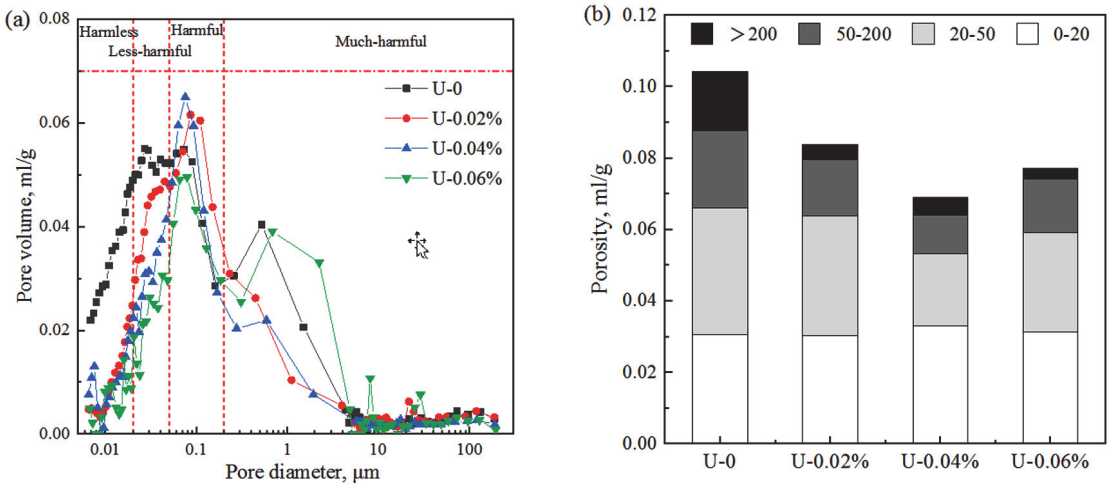

Fig. 10. MIP results of UHPC: (a) pore size distribution, and (b) porosity.

From the above, it can be seen that adding 0.04 % GO can enhance the mechanical properties of UHPC used for bridges and improve its durability, as well as reduce the cracks caused by shrinkage and prolong the service life of UHPC for bridges under the condition that the construction performance of UHPC for bridges is satisfied.

References

1. F.de Larrard, T.Sedran, *Cement Concrete Res.*, **24**, 997 (1994).
2. S.Jie, *Adv. Mater. Res.*, **168**, 1506 (2011).
3. K.Wille, C.Boisvert-Cotulio, *Constr. Buildi. Mater.*, **86**, 33 (2015).
4. H.Yazici, M.Y.Yardimci, S.Aydin et al., *Constr. Buildi. Mater.*, **23**, 1223 (2009).
5. Z.Pan, L.He, L.Qiu et al., *Cement Concrete Composites*, **58**, 140 (2015).
6. S.Lv, Y.Ma, C.Qiu et al., *Constr. Buildi. Mater.*, **49**, 121 (2013).
7. A.Mohammed, J.G.Sanjayan, W.H.Duan et al., *Constr. Buildi. Mater.*, **84**, 341 (2015).
8. A.Mohammed, J.G.Sanjayan, A.Nazari et al., *Constr. Buildi. Mater.*, **168**, 858 (2018).
9. E.Garcia-Taengua, M.Sonebi, K.M.A.Hossain et al., *Composites Part B: Engin.*, **81**, 120 (2015).
10. M.Sonebi, E.Garcia-Taengua, K.M.A.Hossain et al., *Constr. Buildi. Mater.*, **84**, 269 (2015).
11. A.Mohammed, J.G.Sanjayan, W.H.Duan et al., *Construction and Building Materials*, **84**, 341 (2015).
12. H.Peng, Y.Ge, C.S.Cai et al., *Constr. Buildi. Mater.*, **194**, 102 (2019).
13. N.I.Zaaba, K.L.Foo, U.Hashim et al., *Procedia Engin.*, **184**, 469 (2017).
14. L.Yu, R.Wu, *Constr. Build. Mater.*, **259**, 120657 (2020).
15. R.Karim, M.Najimi, B.Shafei, *J. Constr. Build. Mater.*, **227**, 117031 (2019).
16. H.Kim, T.Koh, S.Pyo, *Constr. Build. Mater.*, **123**, 153 (2016).
17. H.Wan, Y.Zhang, *Mater. Struct.*, **53**, 1 (2020).
18. K.Guo, H.Miao, L.Liu et al., *Nanotechn. Rev.*, **8**, 681 (2019).
19. Z.F.Ren, Properties of Ultra High Performance Cement-based Materials Modified by Graphene Oxide [D]. Wuhan University of Technology, Hunan (2018).
20. S.C.Devi, R.A.Khan, *J. Build. Engin.*, **27**, 101007 (2020).
21. H.Chu, J.Jiang, W.Sun et al., *Cement Concrete Composites*, **82**, 252 (2017).
22. B.Zhang, H.Tan, W.Shen et al., *Cement Concrete Composites*, **92**, 7 (2018).
23. Z.He, P.Zhan, S.Du et al., *Composites Part B: Engin.*, **166**, 13 (2019).